# 2-D Light Diffraction from CCD and Intensified Reticon Multichannel Detectors Causes Spectrometer Stray Light Problems

**RICHARD W. BORMETT and SANFORD A. ASHER***
*Department of Chemistry, University of Pittsburgh, Pittsburgh, Pennsylvania 15260*

**Intensified diode arrays and charge-coupled detectors (CCD) which are used as multichannel detectors for spectroscopy exhibit strong 2-D diffraction of light due to the micro-channel plate intensifier and the CCD surface microelectronic structures. The strong 2-D diffraction of light by the intensified diode arrays shows hexagonal symmetry due to the hexagonal packing of the hollow glass fibers of the micro-channel plate intensifier. The 2-D diffraction of light from the CCD detectors shows square symmetry due to the almost square symmetry of the individual surface microelectronic structures. Light incident on the detector surfaces is diffracted into numerous angles which depend upon the incident angle and the light wavelength. This diffracted light can be redispersed and/or reflected and scattered by optical elements inside the spectrometer. This diffracted light can then contribute to spectrometer diffuse stray light or it can be directly reimaged onto the detector to cause spectral artifacts. Backthinned CCD detectors do not show 2-D light diffraction and thus avoid these 2-D diffraction stray light limitations.**

Index Headings: **Raman spectroscopy; Intensified diode array; CCD; Detectors; Stray light.**

## INTRODUCTION

Raman spectral measurements examine the small fraction of light which is inelastically scattered by matter.[1] The Raman scattered light intensities are typically much weaker than the elastically scattered light intensities. Even dust-free pure liquids which show very weak elastic Rayleigh scattering show Raman intensities much more than a thousandfold weaker than the Rayleigh scattered intensity.[1] Particulate matter can result in elastically scattered intensities $10^{10}$-fold more intense than the Raman scattered intensities. Detection of the Raman scattered light typically requires a complex multiple-grating spectrometer to spectrally resolve the inelastically scattered light from the dominating elastically scattered light. The ideal Raman spectrometer would consist of a high-dispersion, low-stray-light single monochromator with a multichannel detector.[2] Minimizing the number of optical elements maximizes the transfer efficiency of the spectrometer, which is important when weak excitation sources are being utilized or weak Raman bands are being detected. The multichannel detector would simultaneously accumulate the entire Raman spectrum with a signal-to-noise ratio determined by the shot noise limit. The assumption is that all light incident on the detector is correctly positioned with a single wavelength incident upon each single small region of the detector surface. In fact, the signal-to-noise ratios can be limited by stray light and/or the presence of spectral artifacts. This was a common occurrence in the past when errors in ruled gratings resulted in high levels of stray light and the presence of grating ghosts.

The stray light level of a Raman spectrometer is typically reported as the fraction of the Rayleigh light that enters the spectrometer which is incident on the detector even though the monochromator grating is set to image this Rayleigh scattering away from the detector. Spectrometers which utilize slits and photomultipliers have stray light contributions which result from diffuse scattering from imperfections on the optical surfaces and from imperfections and limitations of the diffraction gratings. Generally the stray light is dominated by the quality of the gratings, assuming that high-quality optical elements are used and that they have not degraded due to corrosive environments. Typical single-stage spectrometers provide stray light rejections of, at best, $10^{-5}$ to $10^{-6}$.

The stray light problem for a single monochromator is minimized by minimizing the Rayleigh scattered light intensity entering the monochromator. This process involves the use of narrow-band rejection filters when available—for example, holographic edge and notch filters, interference filters, atomic line vapor cells[3] and crystalline colloidal Bragg diffraction filters.[4] Double or triple monochromators are often required for spectral regions where these narrow-band rejection filters are not readily available (for example, in the UV). If the stray light rejection at the Rayleigh wavelength is identical at $10^{-5}$ for both stages of a double monochromator, for example, then the stray light level from Rayleigh scattered light at the detector will be $10^{-10}$. Similarly, a triple monochromator could achieve a stray light level of $10^{-15}$ with respect to the Rayleigh scattered light.

The new generations of spectroscopic multichannel detectors permit dramatic increases in spectral signal-to-noise ratios because they function as an array of shot-noise-limited detectors. They are used in spectrographs where the photoactive elements lie in the spectrograph image plane. The assumption is that they are passive

Received 27 February 1993; revision received 9 August 1993.
* Author to whom correspondence should be sent.


0003-7028/94/4801-0001$2.00/0

devices and act as electronic photographic film. Unfortunately, these detectors are not blackbodies that absorb all the incident light. In contrast, we show here that the intensified photodiode arrays (IPDA) and charge-coupled detector (CCD) can give rise to new sources of stray light which result from the strong 2-D diffraction of light from the microstructures that make up the multichannel detectors. 2-D light diffraction occurs from the hexagonal microstructures of the micro-channel plate intensifiers of the IPDA and from the regular array of microelectronic structures on the surface of the CCD. IPDAs and CCDs are in wide use in spectroscopy since they have high light sensitivity, have a large dynamic range, have a wide wavelength sensitivity, and, in the case of IPDAs, can be gated very quickly.[5] Our results indicate that the improvement in signal-to-noise is ultimately limited by the contribution of 2-D diffraction to stray light and its appearance as spectral artifacts.

## EXPERIMENTAL

We examined the 2-D diffraction from the multichannel detectors by focusing a 0.5-mW He-Ne laser on the surfaces of the multichannel detectors. The 2-D diffraction patterns were obtained with a He-Ne laser beam incident at 16° from the surface normal, and the image was recorded from a white surface approximately 24 cm from the multichannel detector with an imaging system equipped with a macro lens. The relative intensity of each diffraction spot from the EG&G 1456 IPDA was measured by focusing each spot onto a Si photodiode and measuring the photocurrent. The 1152 × 298 CCD surface was photographed with the use of an optical reflecting microscope.

The EG&G 1456 and 1420 IPDA multichannel detectors and the EEV 1152 × 298, the Tektronix 512 × 512, and the backthinned Tektronix CCD arrays were mounted at the image plane of a Minuteman Model 310-SMP one-meter single spectrograph to determine the relative contribution of each detector to the diffuse stray light level of the monochromator. This spectrograph is designed for an exceptionally flat image plane with a large spectral coverage. The stray light was measured over a solid angle of $\sim 1 \times 10^{-3}$ steradians by using a 1P28 RCA PMT, which viewed the imaging mirror. The PMT was placed as close as possible to the spectrometer image plane (within 10 cm). The source was a 10-mW He-Ne laser focused into the entrance slit of the monochromator in such a way that it matched the spectrometer *f*/# of 8.7. We compared the magnitude of the stray light in the presence and absence of each detector placed at the spectrograph image plane center.

## RESULTS

Figure 1 shows schematically the 2-D diffraction pattern observed from the EG&G 1456 IPDA in which the incident beam was incident on the detector while the diffraction pattern was viewed on a white screen placed downfield from the detector. Figure 2 shows the actual diffraction patterns recorded by a camera from the different multichannel detectors. The 2-D diffraction patterns from the EG&G 1420 and 1456 IPDA have hexagonal symmetry (Fig. 2a and 2b), while those from the

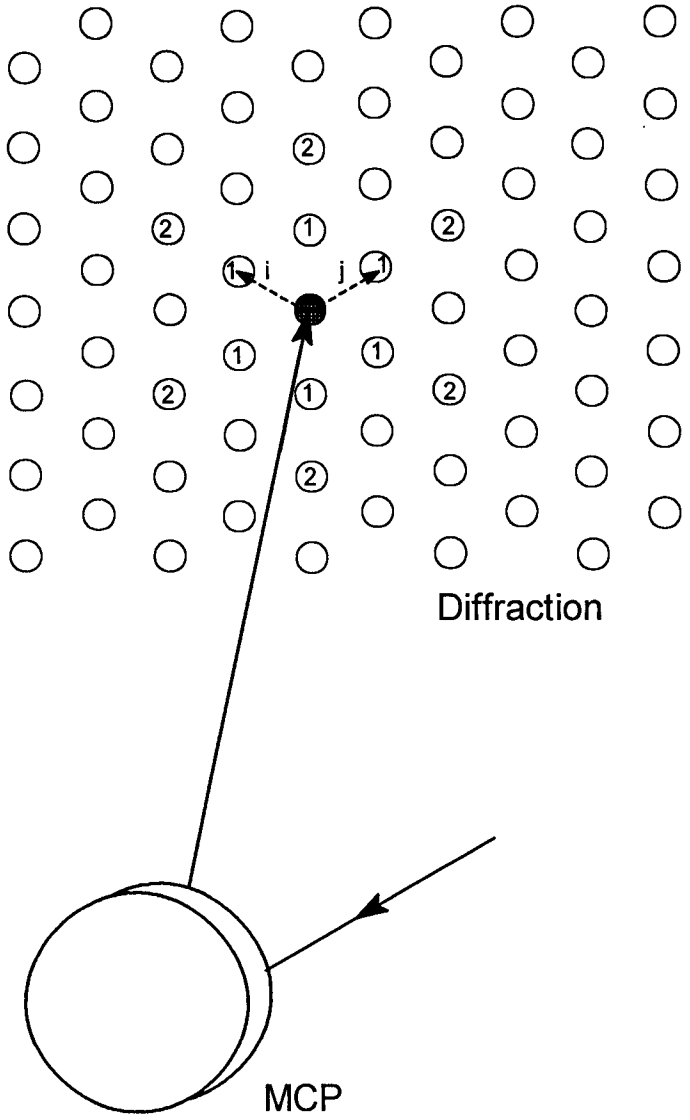


FIG. 1. Schematic representation of the 2-D diffraction pattern observed from micro-channel plate intensifiers with diffraction orders $m = 1$ and $m = 2$ and the lattice vectors $i$ and $j$ labeled.

CCD arrays have square symmetry (Fig. 2c and 2d). These diffraction patterns must result from a hexagonal arrangement of scatterers on the surfaces of the IPDA and a square arrangement of scatterers on the CCD arrays. The backthinned CCD, which is back illuminated, does not show diffraction but specularly reflects 37% of the incident light.

The observed diffraction angles depend both upon the wavelength of light and upon the spacing of the scatterers on the diffracting surface. The 2-D Bragg diffraction equation for a hexagonal array of scatters is:[6]

$$\frac{2m_h\lambda}{\sqrt{3}} = D(\sin\theta_1 + \sin\theta_2). \quad (1a)$$

For the hexagonal array, $m_h$ is defined as $m_h = (m_i^2 - m_i m_j + m_j^2)^{1/2}$.

The 2-D Bragg diffraction equation for the square array is:

$$m_s\lambda = D(\sin\theta_1 + \sin\theta_2) \quad (1b)$$

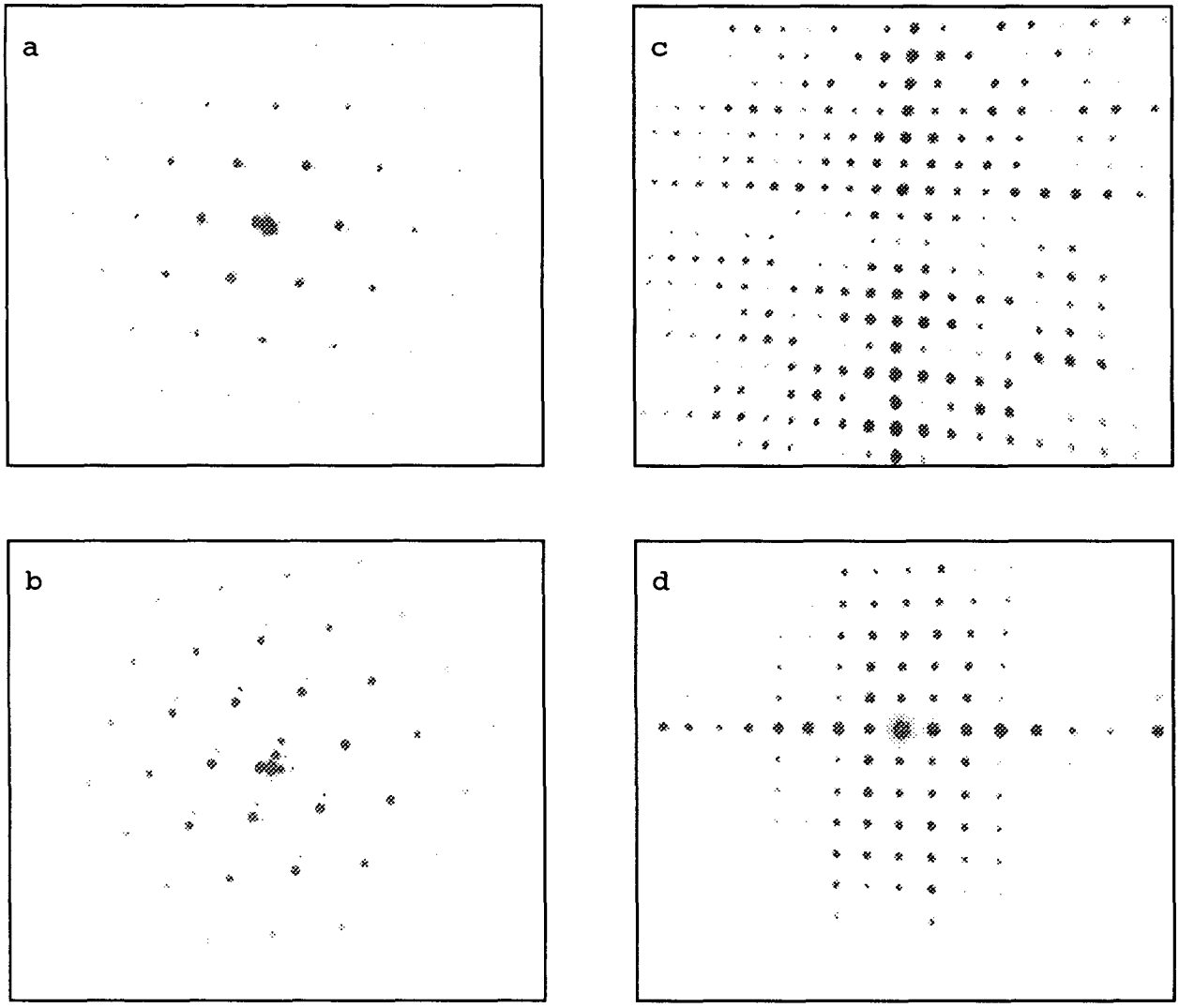


FIG. 2. The 2-D diffraction pattern observed from (**a**) EG&G 1420 IPDA; (**b**) EG&G 1456 IPDA; (**c**) 512 × 512 front Tektronix; (**d**) 1152 × 298 front EEV.

where $m_s = (m_i^2 + m_j^2)^{1/2}$ and $m_i$ and $m_j$ are the integer values of the lattice vectors $i$ and $j$ of the 2-D diffraction array, $\lambda$ is the wavelength of light, $D$ is the spacing between the scatterers, $\theta_1$ is the incidence angle of the light from the normal to the scattering plane, and $\theta_2$ is the diffraction angle.

Table I lists the measured relative intensities observed from the EG&G 1456 IPDA of the Bragg diffracted beams for the first seven integer values of $m_h$. Since the diffraction is sixfold symmetric, the total intensity listed in the table is six times that of each diffraction spot. Most of the intensity (30%) appears in the $m = 0$ spot, which mainly results from specular reflection from the photocathode and the metalized surface of the micro-channel plate. Although not listed, the diffraction intensity of the noninteger values of $m$ (for example, 1.73 and 2.65) is approximately equal to the intensity of the nearest integer value of $m$. Thus, almost 40% of the incident light is reflected or diffracted from the detector back into the spectrometer. The 2-D diffraction occurs from the micro-channel plate, which is behind the photocathode. Thus, approximately 30% of the diffracted light will be reflected by the photocathode back to the micro-channel plate to be rediffracted. This multiple reflection of the 2-D diffracted light from these highly reflective surfaces is also observed in the diffraction pattern when $\theta_1$ or $\theta_2$ does not equal 90°; this multiply reflected light appears as spots slightly offset from the nonreflected 2-D diffracted light (Fig. 2b). We calculate a periodicity of 11 $\mu$m for the diffracting elements for both IPDA detectors.

**TABLE I. Relative intensities of several 2-D diffraction spots from an intensified diode array.**

| $m$ | Relative intensity | |
|---|---|---|
| incident | 100 | |
| 0 | 30.0 | (Reflection) |
| 1 | 1.00 | |
| 2 | 0.19 | |
| 3 | 0.064 | |
| 4 | 0.034 | |
| 5 | 0.020 | |
| 6 | 0.014 | |

The diffraction patterns from both front-illuminated CCD arrays have square symmetry, but the relative intensity patterns of the different spots differ between the CCDs. We calculate a periodicity of 22.5 $\mu$m for the 1152

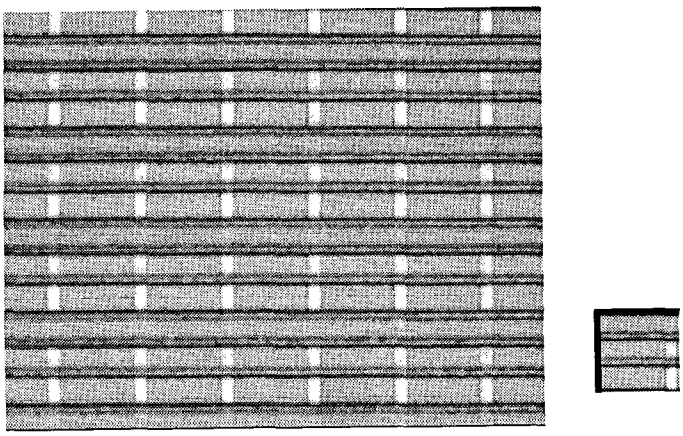


FIG. 3. Micrograph of the surface of the 1152 × 298 CCD with the basis of the square array shown to the right obtained with a 100× objective and 2.5× eye piece.

× 298 CCD and a periodicity of 27 μm for the 512 × 512 CCD. The differences in the diffraction pattern spacings result from the differences in the lattice spacings. The differences in the relative intensities of the spots result from differences in the microstructure of the 2-D diffracting lattice. While it is possible, in principle, to calculate the structure of the diffracting array from the diffraction pattern, it is much easier to visualize it with the use of a reflecting microscope. Figure 3 shows a micrograph of the surface of the 1152 × 298 CCD. This is a square periodic array formed by the array gate structure. The basis for the array is shown to the right of the figure. The other CCD array appears somewhat similar, but the differences which exist cause alterations in the relative intensities of the Bragg diffraction spots. Some patterns are obvious, such as the fact that the diffracted intensities of the spots that are perpendicular to the horizontal stripes of Fig. 3 are stronger than those parallel to the stripes; these stripes dominate the diffraction. Approximately 40% of the incident light is diffracted by the front-illuminated CCD arrays.

Table II lists the change in the stray light detected by the PMT placed at various positions along the image plane of the spectrograph. If the stray light is the result of diffuse scattering from imperfections in the final mirror, for example, there should not be a significant difference in the measured value as the PMT is moved to alternative positions in the image plane. On the other hand, if light from the detector is reflected or diffracted back into the spectrometer, it may be reimaged or redirected back to the image plane to give rise to intense features in the image plane. Table II displays the relative increase in the diffuse and 2-D scattered light observed upon introduction of either a black shutter or one of the detectors in the image plane. The stray light increase listed is that measured relative to the stray light present in the absence of the multichannel detector when the light is permitted to exit the spectrograph. The measured light intensities strongly depend upon the PMT placement. Figure 4 shows the optical arrangement of the spectrograph and the two positions of the PMT, either on the grating side or on the exterior side of the spectrograph.

**TABLE II. Relative increase in the diffuse stray light level from multichannel detectors.**

| Detector | Change in stray light level PMT position (%) | |
|---|---|---|
| | Grating side | Exterior side |
| Shutter | 500 | 0 |
| 1456 IPDA | 475 | 8 |
| 1420 IPDA | 475 | 2 |
| 512 × 512 CCD | 5000 | 20 |
| 1152 × 298 CCD | 2400 | 7 |
| Backthinned CCD | 233 | 1 |

The PMT was placed between 7 and 10 cm off the optic axis that occurred at the center of the multichannel detector. Significantly more intensity was observed on the side towards the grating, since the final mirror recollimates light scattered from the detector or the shutter back towards the grating. For this spectrograph, the light is dispersed on the detector by a high-*f*/# spectrograph, but light scattered or diffracted from the detector is collected at a much lower *f*/#.

The scattered light from the surface of the black shutter causes a 500% increase in stray light on the grating side of the spectrograph. In contrast, the shutter gives no observable intensity increase when the PMT occurs on the exterior side of the spectrograph. The back-illuminated CCD does not diffract but specularly reflects and scatters approximately 40% of the incident light. This pattern results in little stray light increase on the exterior side, but causes a 233% stray light increase on the grating side. The front-illuminated CCD detectors result in significantly more stray light on the grating side, in comparison to the IPDA detectors. The 512 × 512 detector was significantly worse than any other detector. The contribution of the 2-D diffracted light to stray light on the grating side of the image plane was clearly evident by looking into the spectrometer, since the image of the scattered light could be easily observed on a white card placed in front of the PMT.

## DISCUSSION

Micro-channel plate intensified photodiode arrays are designed to provide a $10^3$ to $10^4$ gain prior to detection by a Si photodiode array. The micro-channel plate consists of a densely packed hexagonal array of hollow glass

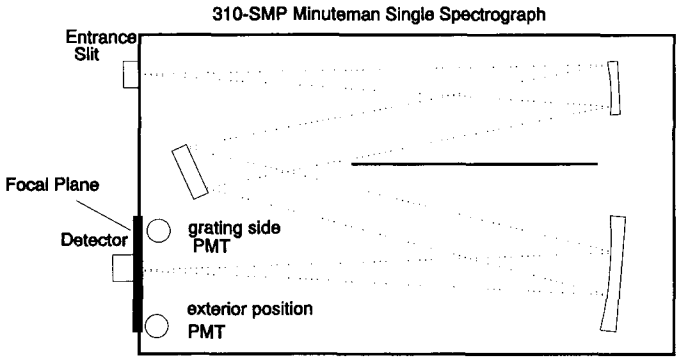


FIG. 4. Optical arrangement of the Minuteman 310-SLM one-meter single spectrograph and the two positions of the PMT used to obtain stray light levels listed in Table II.

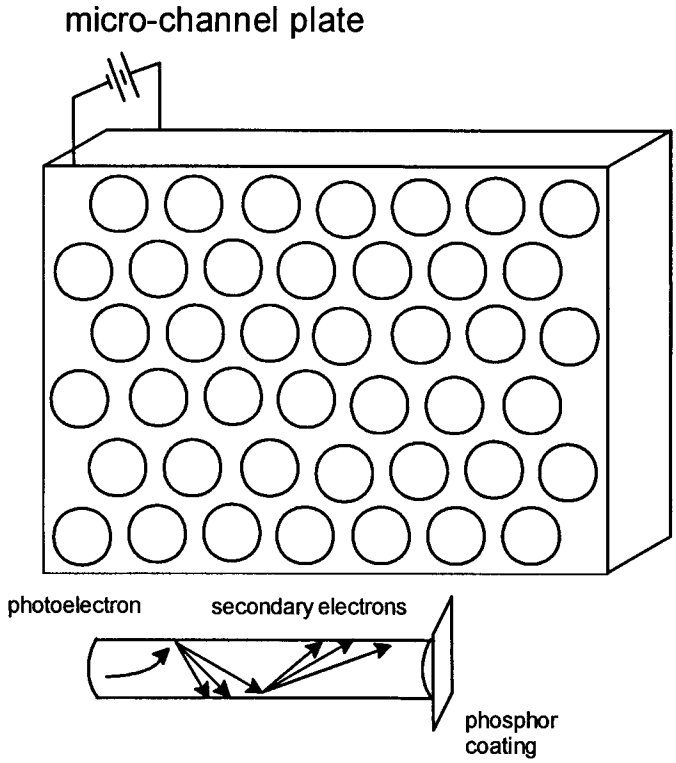


FIG. 5. Arrangement of hollow glass fibers of a micro-channel plate and method of amplification for individual glass fibers of the micro-channel plate.

fibers (Fig. 5). The inside surface of the hollow glass fibers is coated with a low-work-function-resistive material, and the ends of the micro-channel plate are coated with a conductive material across which a large potential difference is applied[7] (Fig. 2a). A very thin transmitting photocathode optimized for the wavelength region of interest is in close proximity to the face of the micro-channel plate. Photons striking the photocathode cause photoelectron emission. Most of the photoelectrons enter the hollow glass fibers and strike the resistive coating, which causes the secondary emission of additional electrons. Since the secondary electrons are confined within the hexagonally arranged micro-channels, spatial information is maintained. After exiting the micro-channel plate, the electrons are accelerated towards a phosphor screen. The resulting photons are coupled with a fiber-optic bundle to the photodiode array.

The diffraction from the IPDA occurs from the hexagonal array of hollow glass fibers. The diffraction results in redirection of part of the spectrometer-dispersed light back into the spectrometer. This light may then be reflected or scattered from other optical elements and be reimaged onto the detector to cause a stray light background or spectral artifacts. In addition, the IPDA has a unique internal stray light problem associated with the reflection by the photocathode of a significant fraction of the light diffracted by the microchannel plate. We commonly observe phenomena from our IPDA when illuminated by narrow intense sources that appear to be from light channeled across the detector surface. It is possible that this observation results from multiple diffractions and reflections between the photocathode and the micro-channel plate.

Charge-coupled detectors are a class of solid-state charge transfer multichannel detectors that utilize inter-cell charge transfer and ultra-low noise readout of the photogenerated charge.[8] The CCD's ultra-low noise readout characteristics, along with its high dynamic range and high quantum efficiency in the visible wavelength regions, have led to widespread application of these detectors to spectroscopic and imaging instruments. CCDs utilize metal-oxide-semiconductor gates fabricated above the photosensitive area to store and transfer the accumulated photogenerated charge. From the microscope image of the CCD surface (Fig. 3) both the 1152 × 298 and the 512 × 512 CCD appear to utilize a three-potential gate structure, with a size and spacing that matches the size of a single detector element.[8] The 2-D diffraction of light from the CCD occurs from these surface gate structures. Alternatively, a backthinned CCD can be manufactured where the CCD substrate is thinned in order to allow illumination from the side opposite the gate structure (back illumination).

The 2-D diffracted light from the multichannel detectors presents unique stray light problems since the diffraction angles are very wavelength dependent (Eq. 1). Whether the diffracted light returns to the spectrometer mirrors and gratings or strikes a nonoptical surface such as the wall or edge of an optic depends on the *f*/# of the spectrometer and the wavelength of the diffracted light. A micro-channel plate with an 11-$\mu$m spacing will diffract the lowest order of 500-nm light at a 6° angle. Since an *f*/10 spectrometer has a solid collection angle of 5.7°, the diffracted light should not be directed back onto the spectrometer optics. However, the detector is often tilted slightly off the image plane to direct the specularly reflected light from the photocathode away from an optical surface. Thus even for an *f*/10 spectrometer, the diffracted light may be incident onto the spectrometer mirrors and gratings. The situation becomes even worse for the CCDs since they produce much stronger diffraction intensities with a much larger number of closely spaced diffraction orders in comparison to the IPDAs. Any light diffracted onto these mirrors or gratings can make its way back to the detector and can interfere with other bands of interest and appear as ghost-like peaks. The diffracted light that is not recollected by the focusing mirror can contribute to the background stray light level when it is scattered from a spectrometer wall or optical mounts. The increased background light level of the spectrometer decreases the effective dynamic range of the detector. Since there is a wavelength dependence to the diffraction angle, the stray light effects will be highly wavelength dependent and difficult to identify.

The dynamic range of the IPDA and CCD detectors is determined by the smallest and largest signals that can be simultaneously measured by the detector. For an ideal diode array detector or CCD, the dynamic range would be determined by the dynamic range of the individual diodes. In the absence of stray light, the dynamic range of the individual diodes is limited at low light levels by the number of thermally generated electron-hole pairs that occur in the photodiode or by the system readout noise. The dynamic range is limited at high light levels by the saturation level of the photodiode or preamplifier. The dynamic range could be larger than $10^4$ for an IPDA

and $10^6$ for a CCD.[7] Unfortunately, the observed dynamic range of the IPDA and CCD instruments is always lower because of internal scattering or reflection of light at the interfaces of the detector components.[7,8] For example, with an IPDA the detector window, photocathode, microchannel plate, phosphor, fiber-optic bundle, and photodiode array will internally scatter or reflect light to other areas of the detector. The internal reflection and scattering of light limits the ability of the detector to detect weak signals in the presence of much stronger signals. In addition, reimaging of the diffracted light leaving the detector by the spectrometer back onto the detector adds to the potential stray light background.

This 2-D diffracted light cannot be eliminated as a source of stray light in an IPDA and a front-illuminated CCD detector since it is produced by the light incident on the detector. However, the backthinned CCD eliminates 2-D diffraction. This factor may be a compelling reason to prefer a backthinned CCD detector to an intensified diode array when the quantum efficiencies are identical and when the noise is limited by shot noise. The significant level of stray light that occurs as a result of 2-D diffraction from multichannel detectors and the potential for it to interfere with spectral measurements must be considered when one is selecting multichannel detectors. Furthermore, any windows that are used between the spectrograph and the detector should be antireflection coated to minimize multiple reflection of the detector-reflected or -diffracted light.


## ACKNOWLEDGMENTS

We gratefully acknowledge Professor Patrick Treado's help in imaging the diffracted light and in taking the photomicrographs. We thank Yair Talmi and Chris Meyers from Princeton Instruments for supplying the CCD detectors used for these studies. This work was supported by NIH Grant R01-GM 30741-11.



1. (a) D. A. Long, *Raman Spectroscopy* (McGraw-Hill, New York, 1977); (b) S. A. Asher, Anal. Chem. **65,** 59A (1992).
2. S. A. Asher, Ann. Rev. Phys. Chem. **39,** 537 (1988).
3. M. J. Pelletier, Appl. Spectrosc. **46,** 395 (1992).
4. P. Flaugh, S. E. O'Donnell, and S. A. Asher, Appl. Spectrosc. **38,** 847 (1984); S. A. Asher, P. L. Flaugh, and G. Washinger, Spectroscopy **1,** 26 (1986); R. Indralingam, J. B. Simeonsson, G. A. Petrucci, B. W. Smith, and J. D. Winefordner, Anal. Chem. **64,** 964 (1992).
5. *Multichannel Image Detectors,* ACS Symposium Series 102, Y. Talmi, Ed. (American Chemical Society, Washington, D.C., 1979).
6. I. M. Krieger and F. M. O'Neill, JACS **90,** 3114 (1968).
7. R. K. Chang and M. B. Long, in *Light Scattering in Solids II, Topics in Applied Physics,* M. Cardona and G. Güntherodt, Eds. (Springer-Verlag, Heidelberg, 1982), Vol. 50, pp. 179–204.
8. R. B. Bilhorn, J. V. Sweedler, P. M. Epperson, and M. B. Denton, Appl. Spectrosc. **41,** 1114 (1987).